Using the VolksMeter

1 Display choices

The raw data output is the preferred display for viewing local earthquakes. For observers in earthquake prone country such as California, it is the natural one for the helicord display. Teleseismic earthquakes show up better in real-time when looking at the integrated-data output.

A useful operating mode is one in which the raw data and integrated data are simultaneously visible on separate windows of the monitor as illustrated in Fig. 1. In the foreground is a 12-h helicord display of the integrated data (channel 3). The background window (which can be brought to the foreground by clicking on it with the left mouse button) is the single line display showing the last 4-h of the raw data, channel 1.

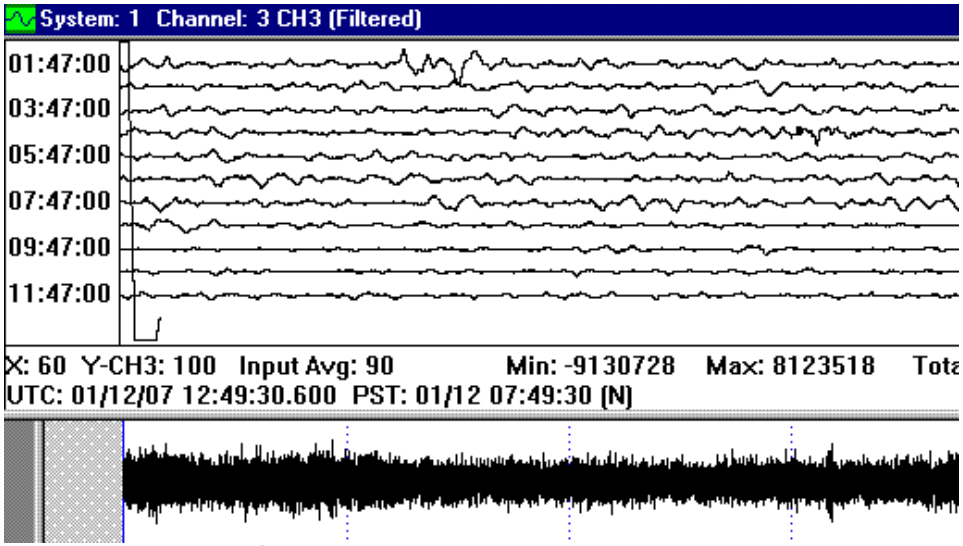

Figure 1. An example of two channels being simultaneously displayed on the computer monitor. The 12-h helicord is the foreground window, whereas the single-line display is the window in the background.

1.1 Local earthquake example

Shown in Fig. 2 (bottom graph) is an earthquake that occurred 75 km from the instrument located in Redwood City, CA. The top graph is the spectrum generated from the data of the lower graph. It is always necessary to do a high-pass filter operation on the raw data before doing the spectrum. The corner frequency for this filter should be as low as possible without introducing a signficant `wave artifact' at the start of the filtered signal. This is easily selected by trial and error; i.e., guess a corner frequency, do the filter and see if the usually-present secular term (drift) has been removed without also introducing the artifact. If there is an artifact, then undo the filter, increase the corner frequency and try again-until a satisfactory result is obtained.

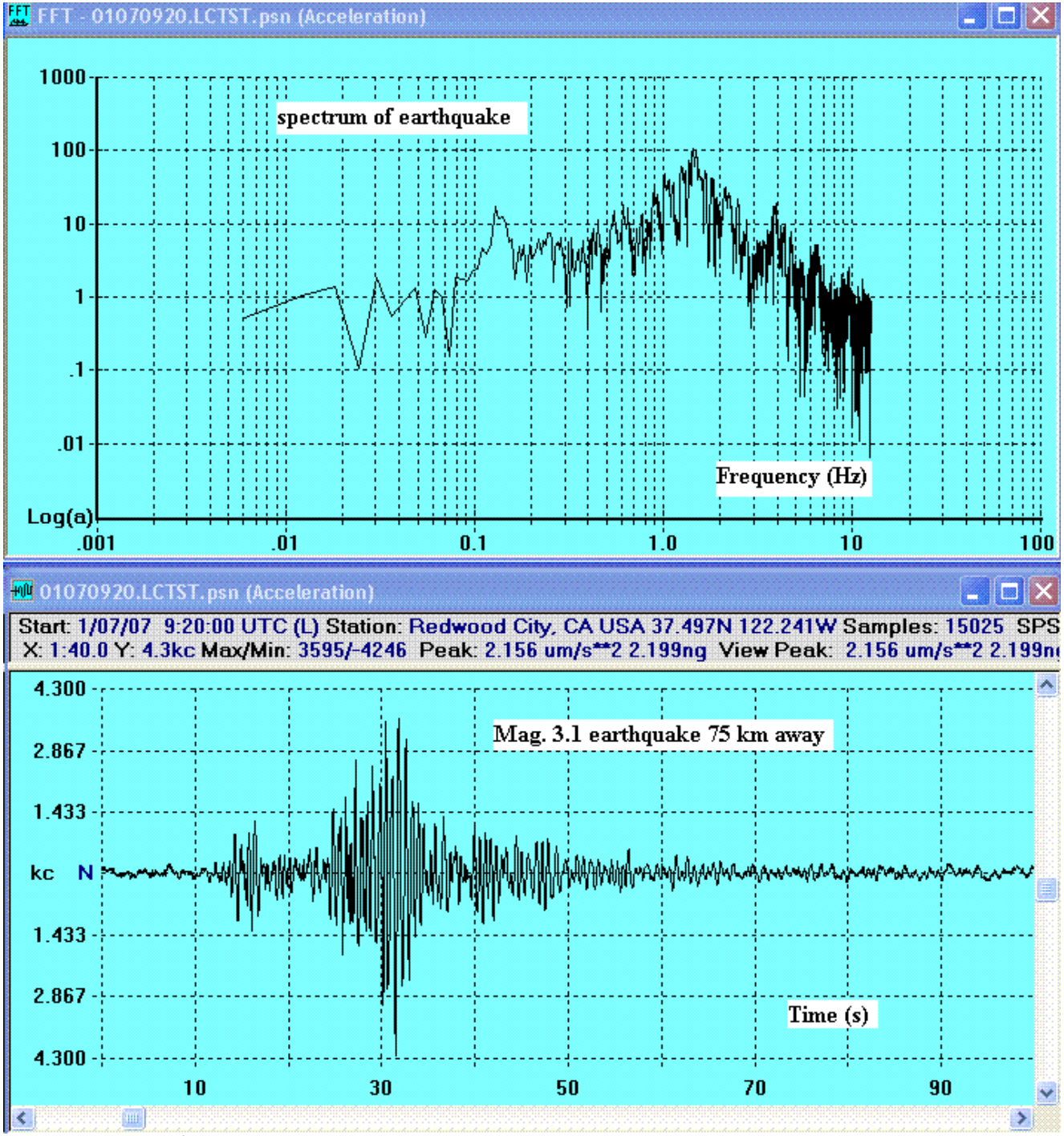

Figure 2. Example of a local earthquake record and its associated spectrum.

1.2 Power spectral density example

As noted in the theory section of this manual, the spectrum of a record is never a faithful representation of the ground-motion power that generated the record. On the other hand, the (specific) power spectral density that does properly represent the ground power is easily generated from the spectrum, by accounting for the transfer function of the instrument. Examples of both the spectrum and the PSD are provided in Fig. 3, which shows not only information corresponding to Fig. 2, but also an estimate of the `background'. The background was obtained by selecting a quiet-time section of the same data channel at an earlier time.

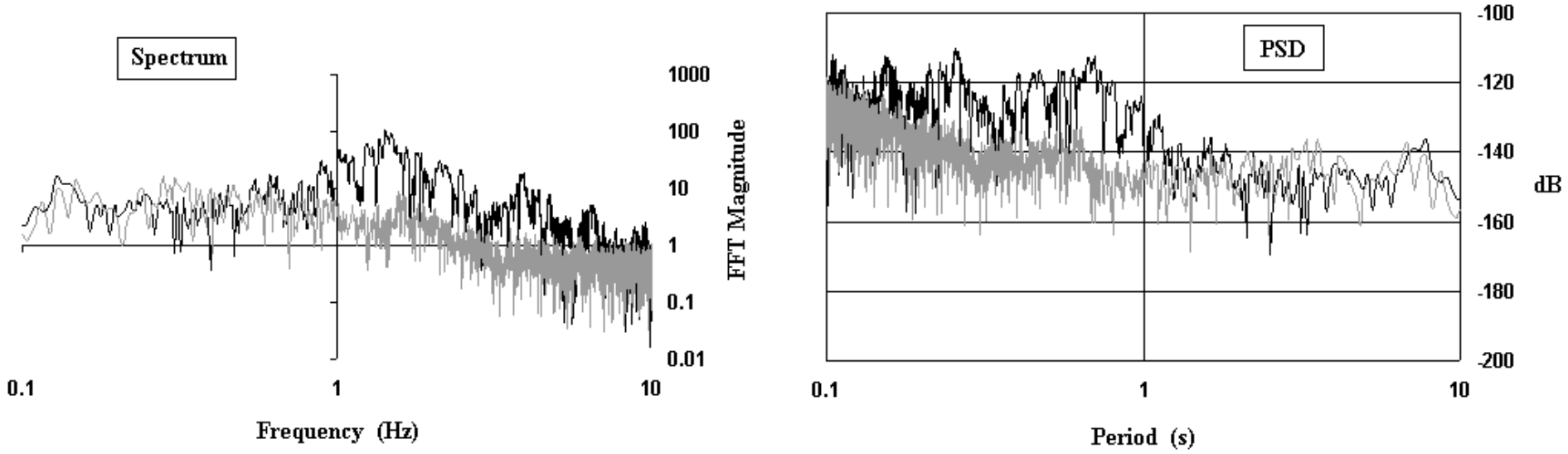

Figure 3. Comparison, for the data of Fig. 2, of (i) spectral data (left) to (ii) the power spectral density (right).

2 Real-time recognition of teleseismic events

As noted earlier, the integrated signal is the channel of preference to make weaker teleseismic earthquakes visible on the helicord. The integral is done numerically by the WinSDR software, after first doing a high-pass filter operation using a low-corner-frequency value. The high-pass filter is a necessary prerequisite, as was also true for doing the FFT on a raw data record. If the corner-frequency of this filter is too high, then the benefits of integration are reduced. On the other hand, if it is too low, then artifacts are introduced. As compared to the raw data channel, the integrated channel is not as quantitatively reliable, for reason of artifacts that occur in the lowest frequency components of the integrated signal. Fig. 4a illustrates the enhancement to be realized by the integrated channel when viewing a distant earthquake.

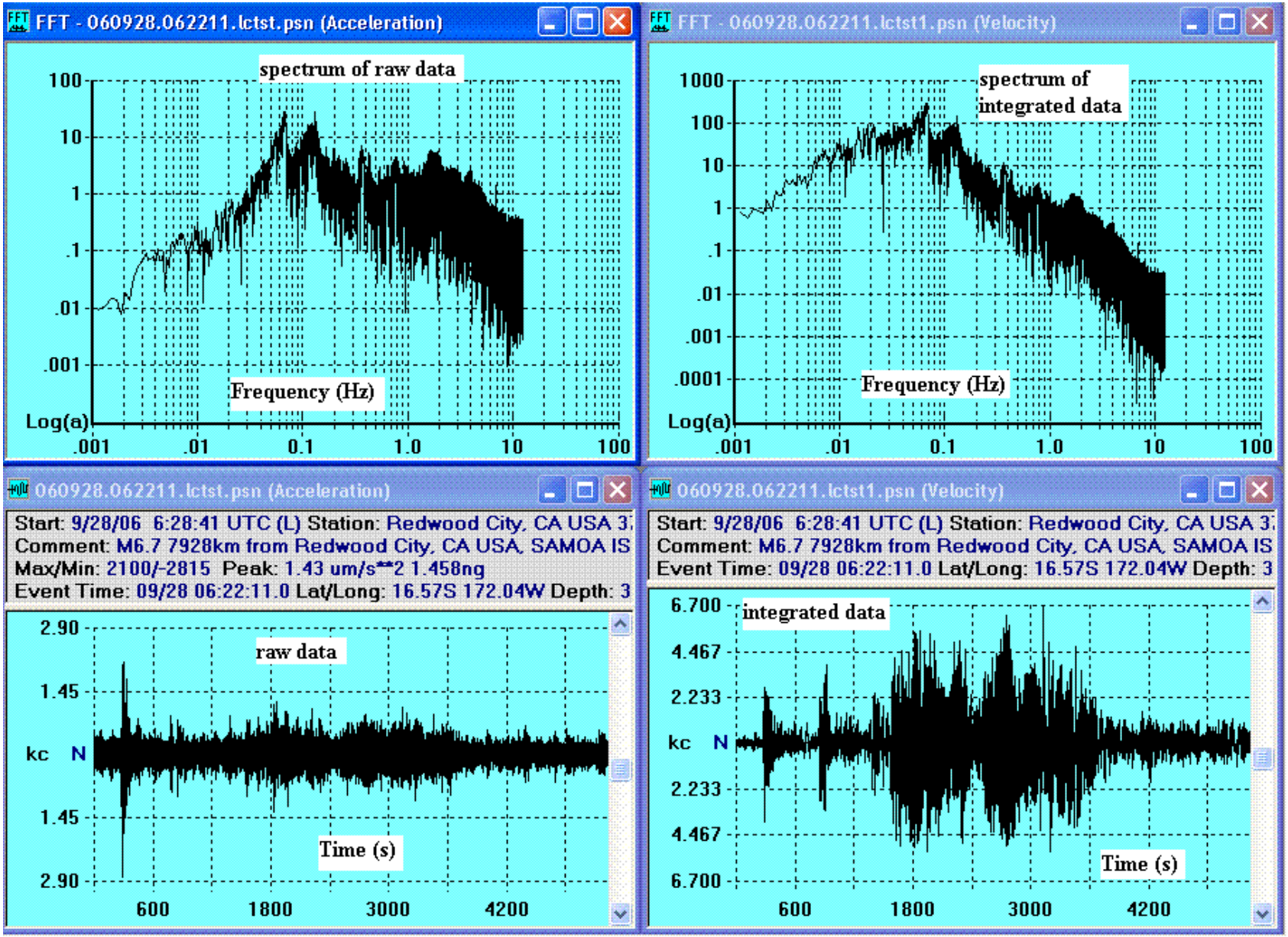

Figure 4a. Comparison of a raw-data channel and its integrated output for purpose of improving the visibility of a teleseismic earthquake in the real-time helicord display. The event of this case corresponds to the Mag. 6.7 earthquake that occurred in Samoa on 28 Sep 06.

Improvement in the signal to noise ratio SNR of the integrated signal trace is immediately obvious by comparing the two lower graphs. The reason for the improvement is that the lower frequencies of the spectrum have been `elevated' as compared to the higher ones. This is a natural consequence of the integration process. It is also possible to improve the SNR of the teleseismic record by removing much of the local noise with a low-pass filter operation; the corner-frequency of the filter needs to be above the dominant components of the earthquake; 0.5 Hz is usually a reasonable choice.

The reason these enhancement methods work is because the largest components of teleseismic waves are of surface-wave type (Rayleigh and Love), with periods usually longer than about 10

s. On the other hand, local earthquakes generate body waves with periods that are usually shorter than about 1 s.

It is worth noting - that the integrated data approximates the signal generated by a broadband seismometer with velocity sensing-for records of teleseismic type. This is true because the VolksMeter is behaving as an accelerometer for drive frequencies below 0.92 Hz (and the integral of acceleration is velocity). For local events in which the drive frequencies are greater than 0.92 Hz, the integrated data attenuates the earthquake record as compared to the raw data; and the integral does not approximate velocity. This is illustrated in Fig. 4b.

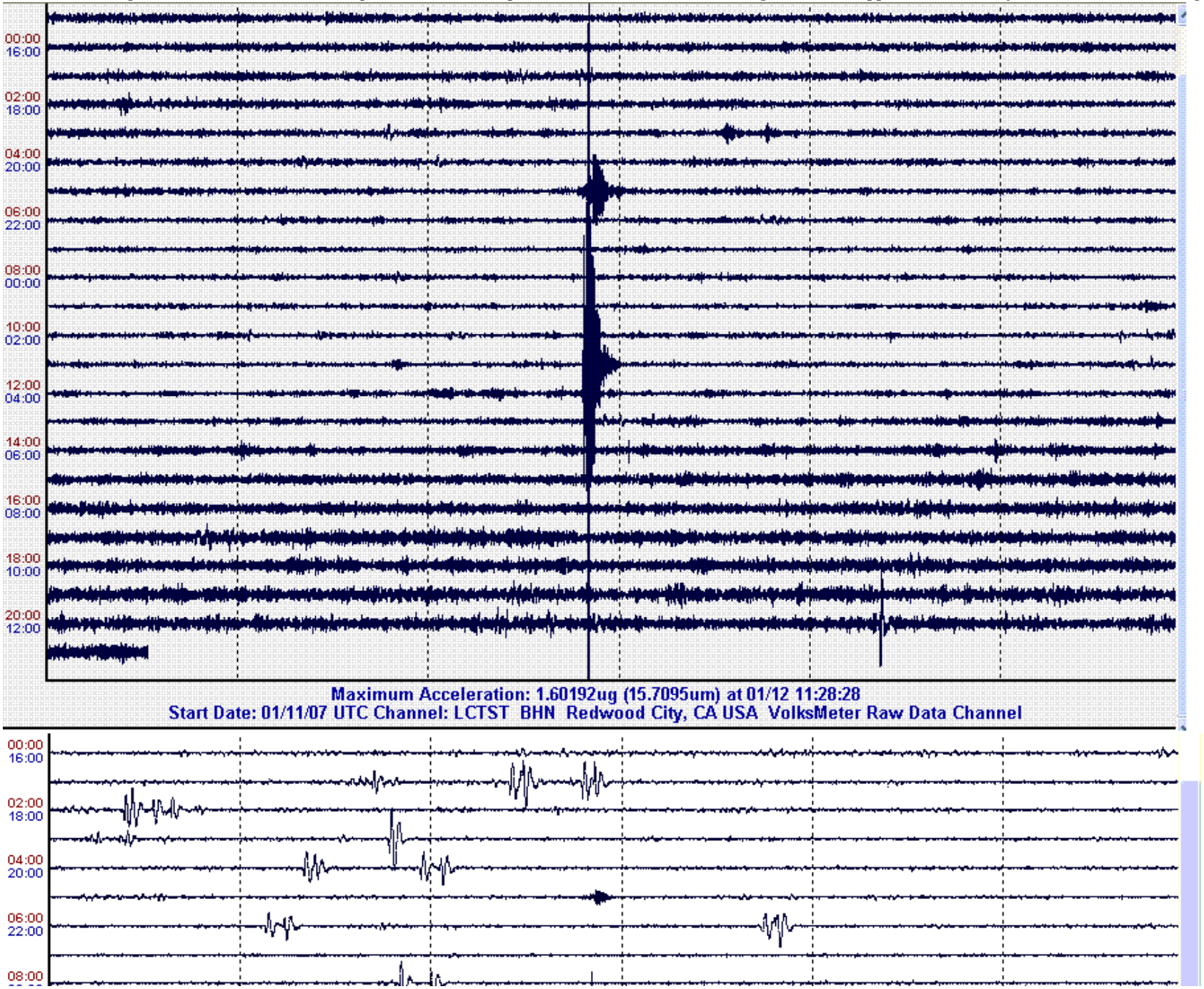

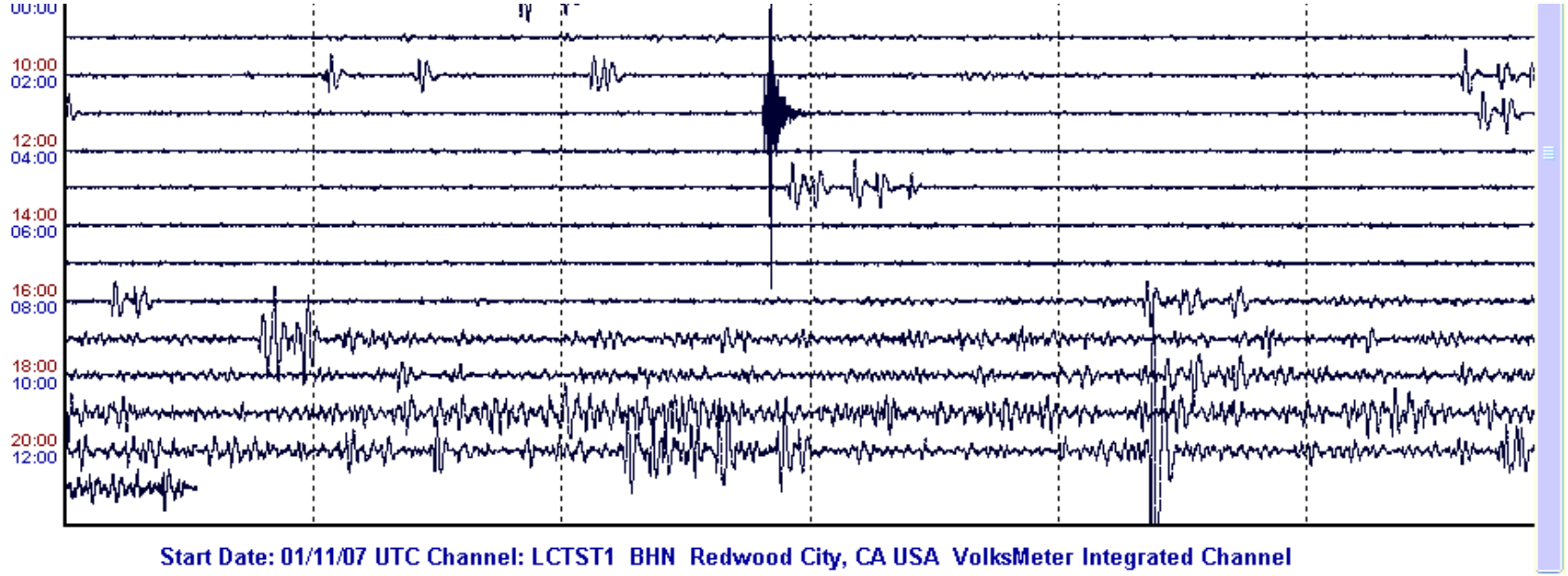

Figure 4b. Helicord comparison of a raw-data channel and its integrated output in the case of a local earthquake. The attenuation that makes the integrated data undesirable is clearly evident.

Another example of the advantage of the integrated signal for teleseismic viewing is shown in Fig. 5. At the bottom of the figure the PSD has been shown for the Kuril Islands earthquake, and also for the Samoa earthquake shown above in Fig. 4.

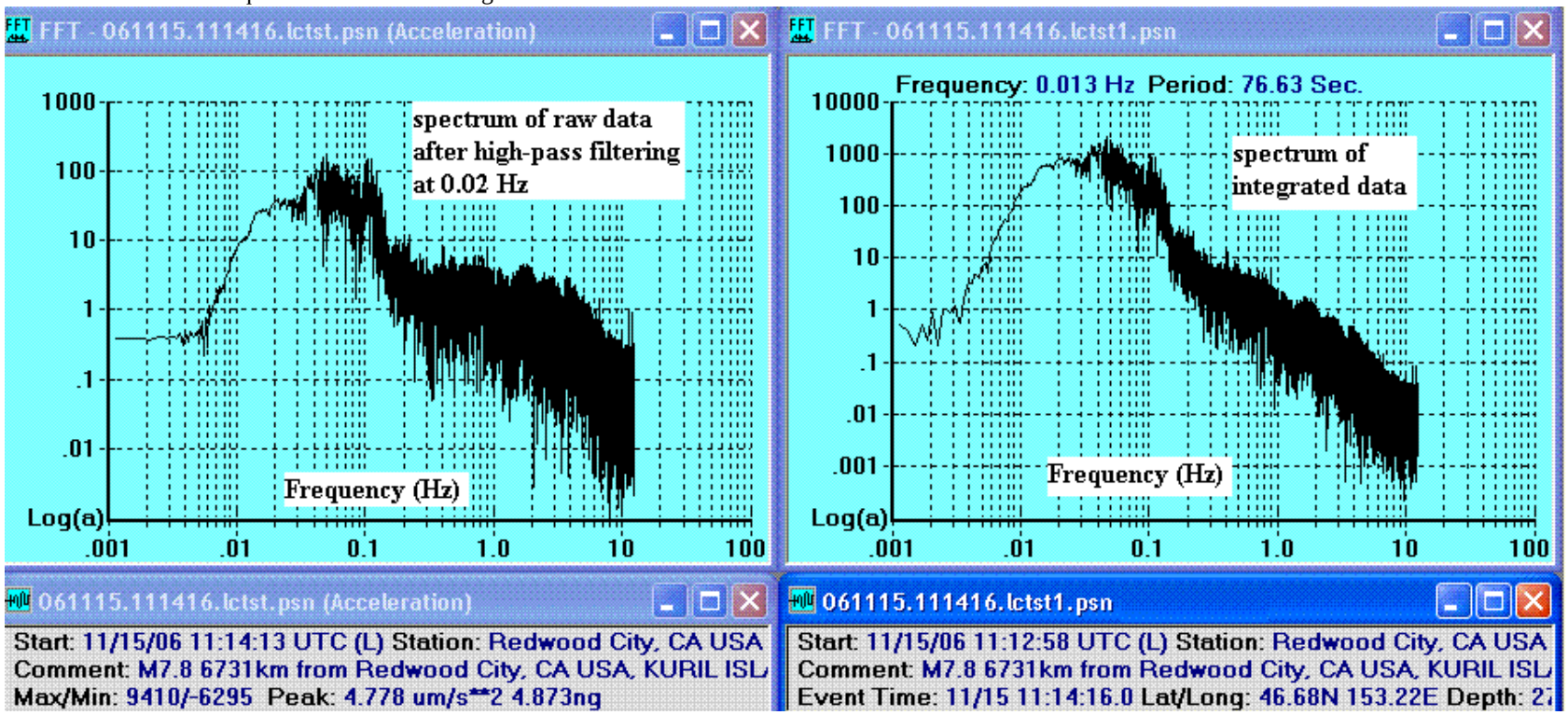

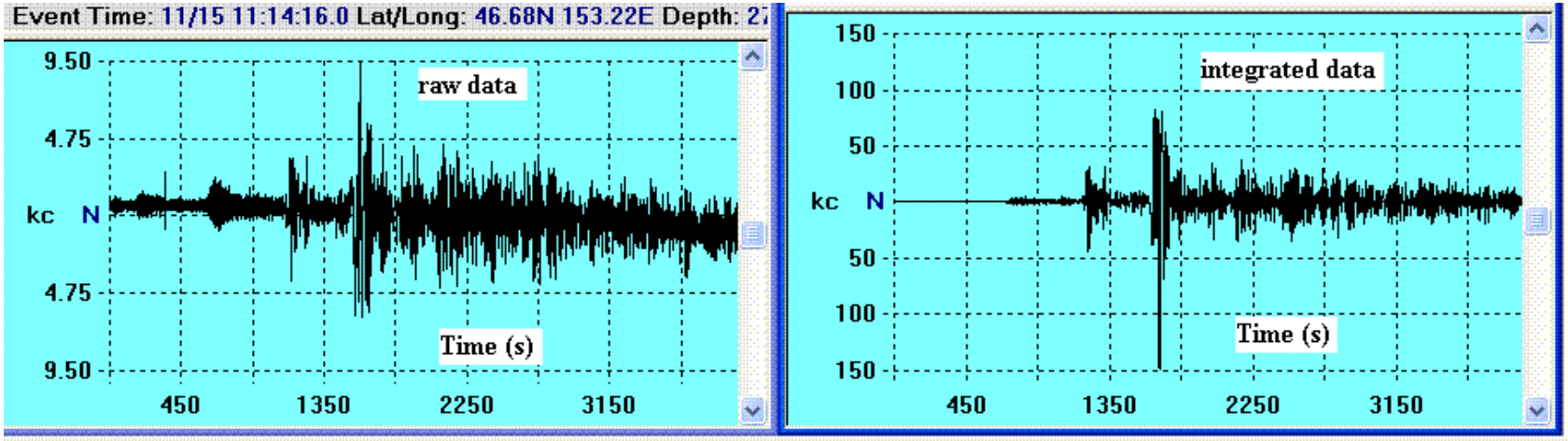

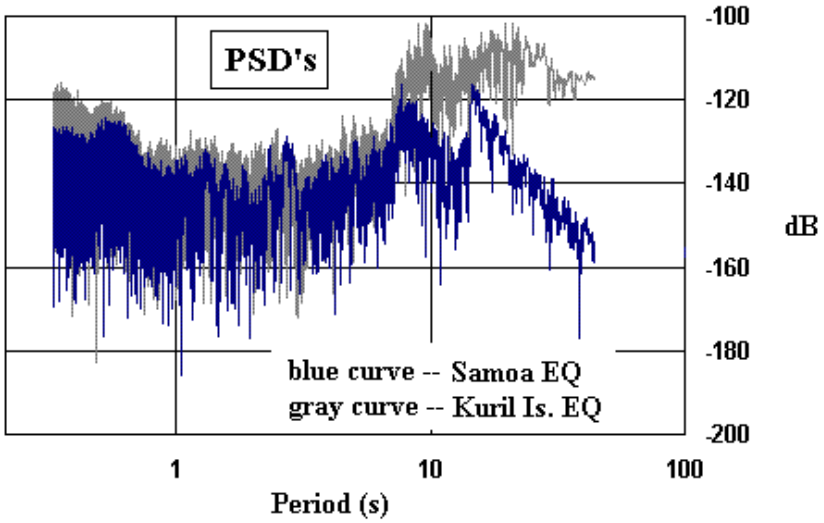

Figure 5. Graphics similar to Fig. 4, corresponding to the Mag. 7.8 Kuril Islands earthquake of 15 Nov 06.

A comparison of the spectral features of the two earthquakes is provided by the PSD's at the bottom of Fig. 5.

3 Two-pendulum instrument advantage

One of the greatest benefits of a VolksMeter equipped with two orthogonal pendulums is its ability to look at correlated output from the pair, as shown in Fig. 6.

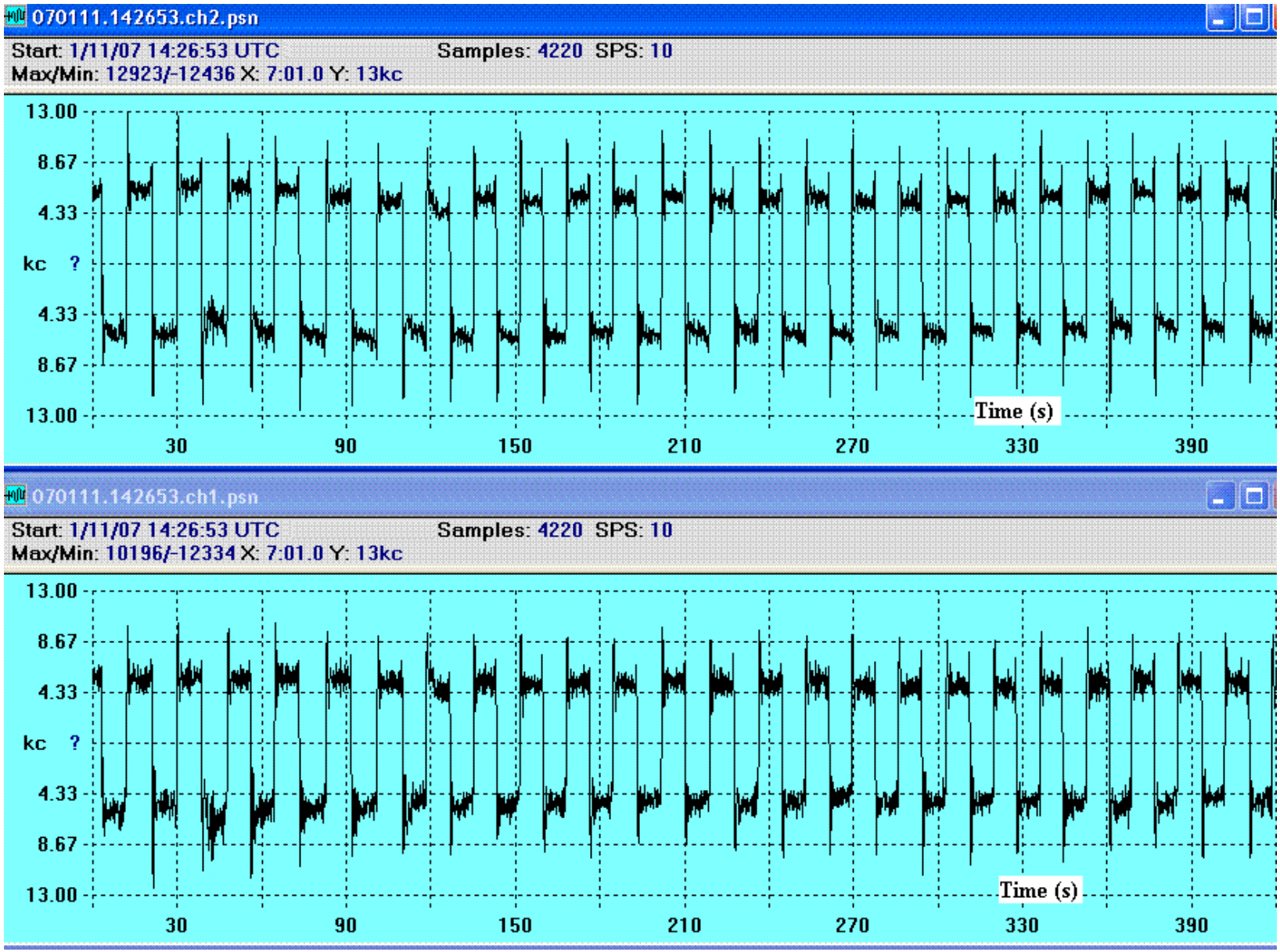

Figure 6. Correlated response of the VolksMeter's two pendulums being driven by a square-wave tilt.

In this case the drive was by means of body-weight, by stepping back and forth between opposite close-positions to the instrument on the concrete-slab floor (on a line diagonal to the square of the case). The deformation of the concrete is seen to be essentially elastic, yielding an amplitude of 5800 ADC counts for the resulting square wave whose period is 17 s. The calibration constant of the pendulums, at 2.5 Gcts/rad yields a tilt amplitude of 2.3 μ rad.

To generate a correlation plot from the pair of WinQuake records shown in Fig. 6, the data were saved as text files and exported to Excel. With Excel several graphs were generated as shown in Figures 7 and 8.

Position data

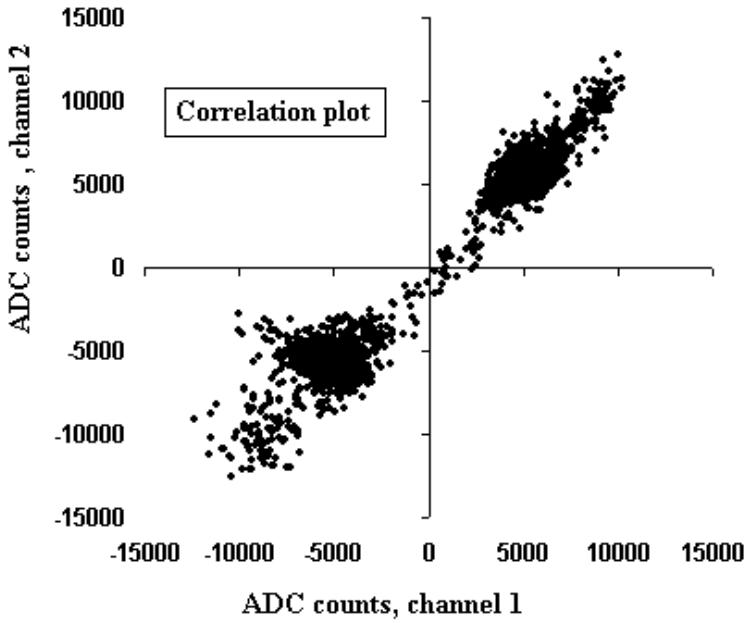

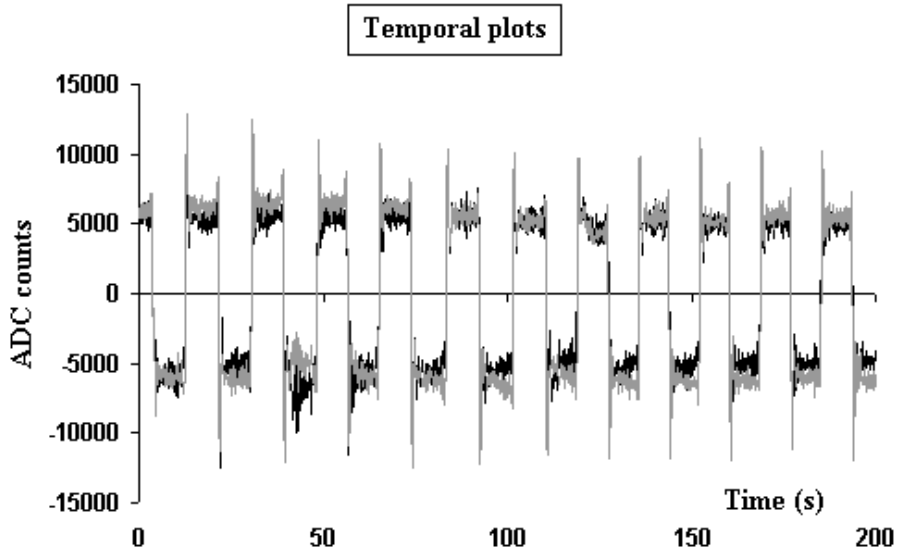

Velocity data

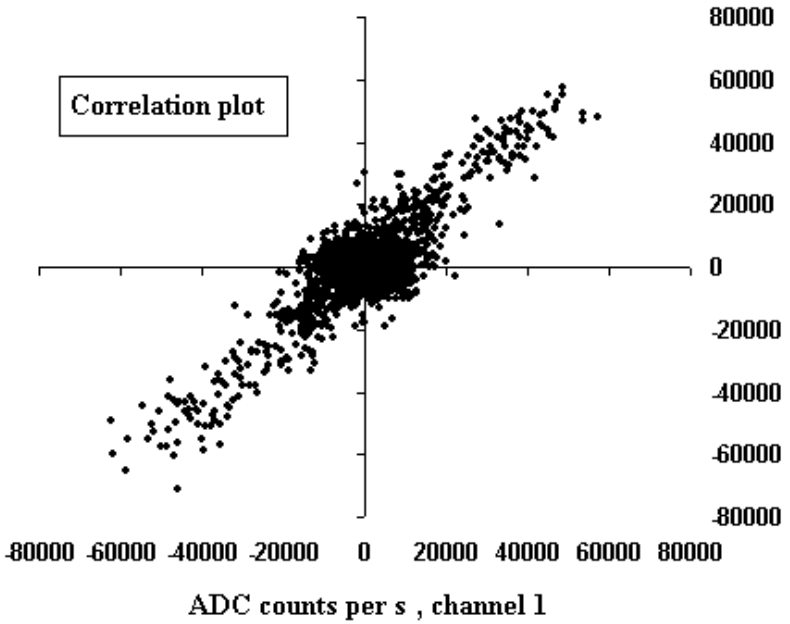

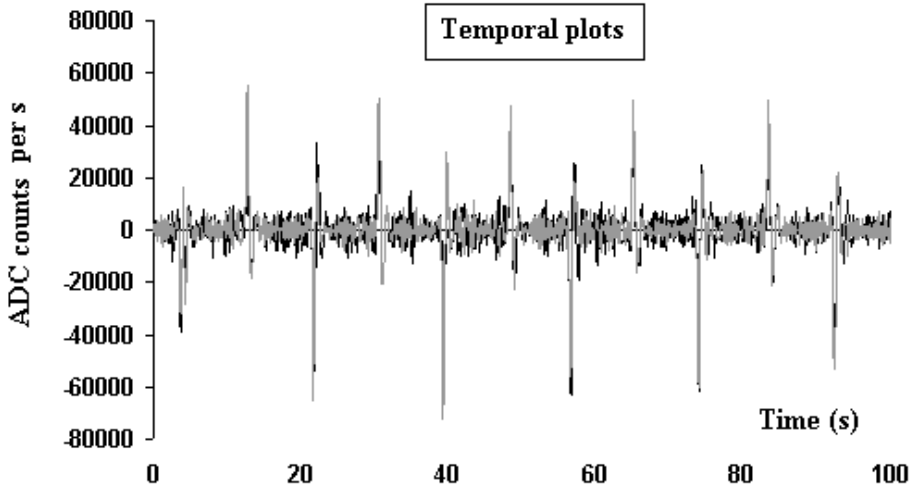

Figure 7. Correlation plots (left graphs) and temporal plots (right graphs) generated with Excel from the data shown in Fig. 6. The velocity results (lower pair of graphs) were obtained by doing a numerical derivative of the position data of the top pair.

Correlated motions of the two pendulums allow one to pass better judgment on the nature of unusual records. In particular, electronic artifacts and/or pendulum anomolous behavior can be ruled out as the cause for the record, when the two channels are showing identical features.

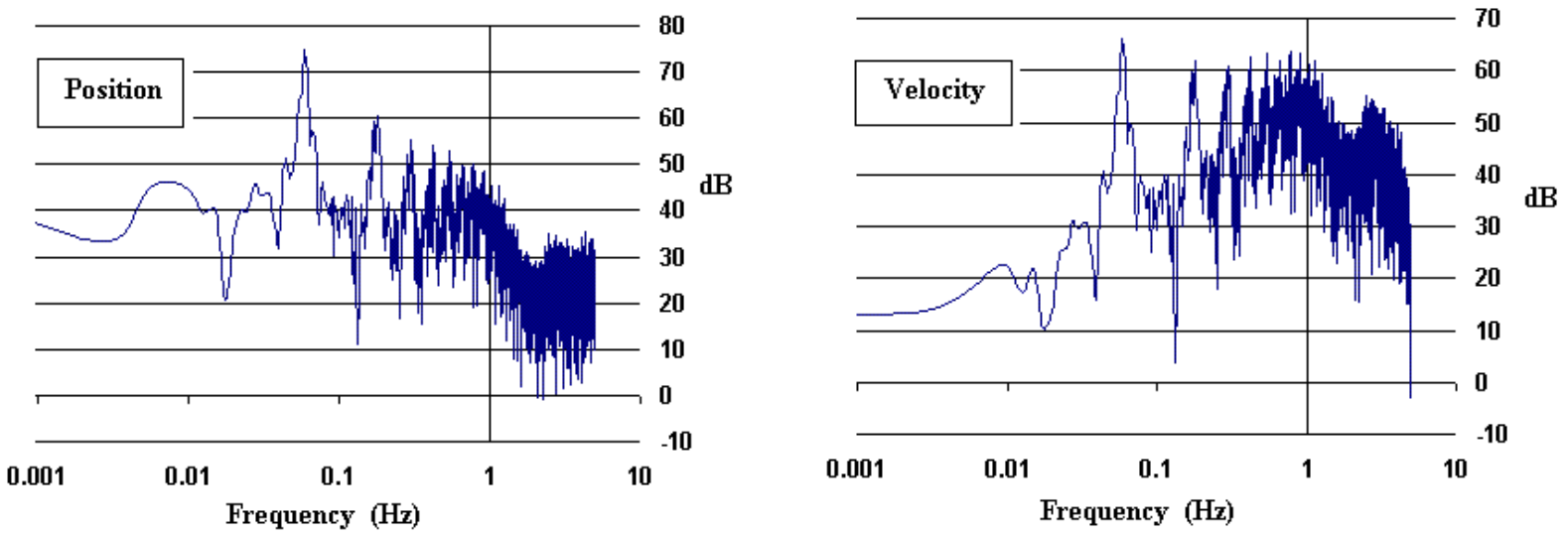

Figure 8. Spectra obtained by doing the Excel FFT on the position and velocity data represented in Fig. 7.

Figures 7 and 8 demonstrate the advantage of position sensing over velocity sensing. For one thing, use of a velocity sensor results in the loss of information. For example, it is not immediately obvious from the velocity record that the drive is a square wave. One can deduce this from the velocity spectrum by noting the presence of odd-harmonics along with the fundamental, which has a frequency of 59 mHz. Notice, however, that the higher frequency components in the velocity spectrum are close to the same intensity in dB as the fundamental. By contrast, in the position spectrum the higher frequencies fall to progressively lower levels with increasing frequency. This is consistent with what is proven in the theory section of this manual; i.e., that a position sensor outperforms a velocity sensor for drive frequencies below the natural frequency of the seismometer.

4 Advantage of Position over Velocity Sensing

The theory section of this manual speaks to the improvement in instrument- generated noise of a postion sensor over a velocity sensor at low frequencies. Concerning Figures 7 and 8, it was also noted that velocity data is afflicted with an inherent loss of information. To further illustrate this loss, consider the time trace shown in Fig. 9.

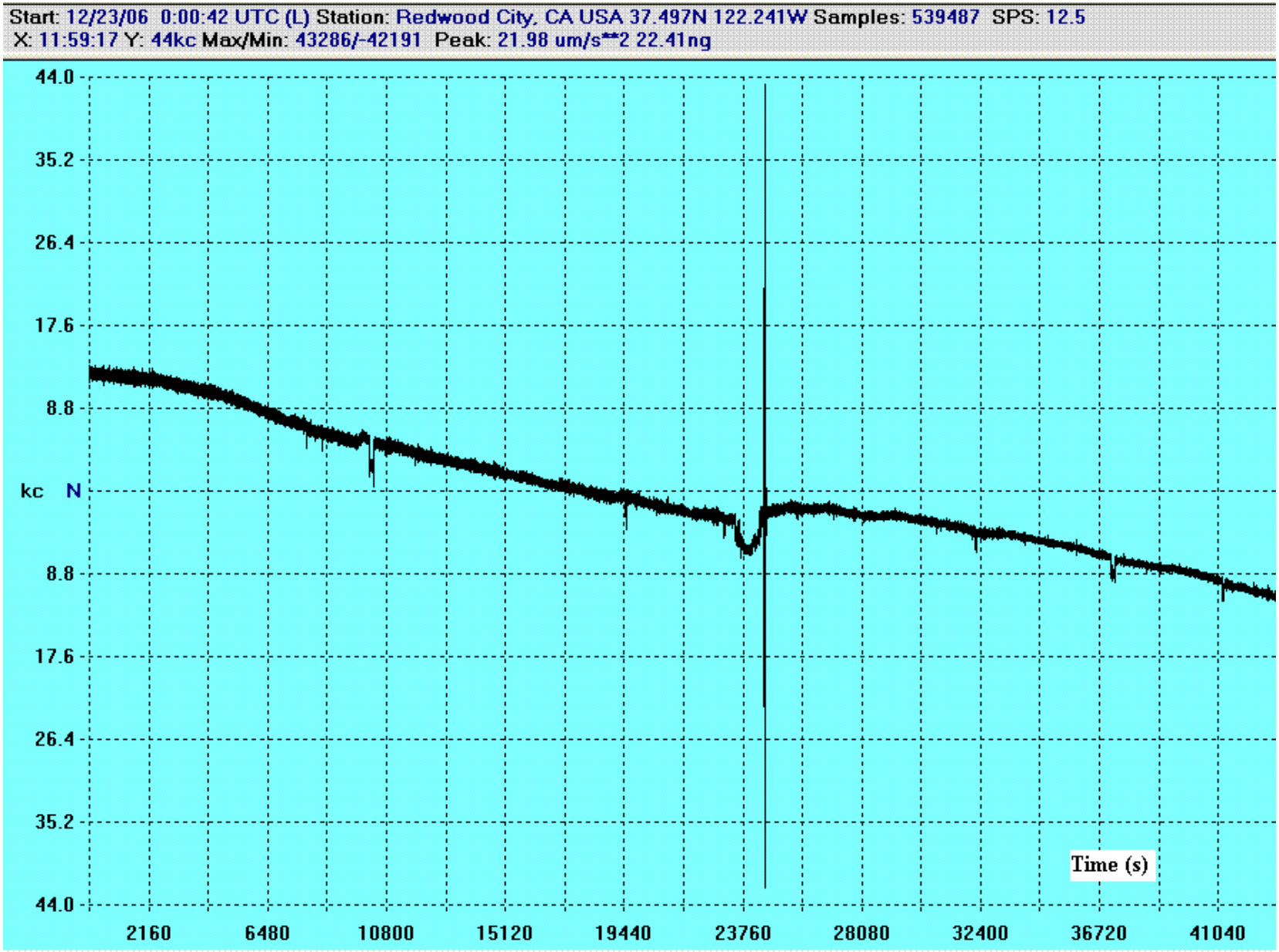

Figure 9. Raw data VolksMeter trace showing an offset before the local earthquake (large sharp lines) observed in the record.

The position data of this figure is seen to have a secular (drift) feature that some may view as undesirable. Some of the drift is probably the result of temperature change of the room housing the seismograph, since the thermal coefficient of the AD7745 is stated in the spec sheet to be 26 ppm of full-scale per Celsius degree (440 ADC counts/C, 24 bits). For the VolksMeter, which uses four capacitors in a symmetric differential configuration, some early tests suggest that the thermal coefficient may be approximately four times the spec value; i.e., 1800 cts/C at 24 bits.

The biggest source of the smooth secular change in Fig. 9 is thought to derive from building tilt, much of which is no doubt thermoelastic in origin. In other words, there is a diurnal variation associated with sunshine. None of these features would be readily discernible if the sensor of the VolksMeter were a velocity type. Although compensation for temperature change may be possible by means of components built into the chip, no such compensation presently exists for the instrument. If the user is interested in record lengths of many hours, it is important to make

the environment of the instrument as close to isothermal as possible.

In Fig. 10, the x-scale has been altered to highlight the offset and the earthquake that immediately follows it.

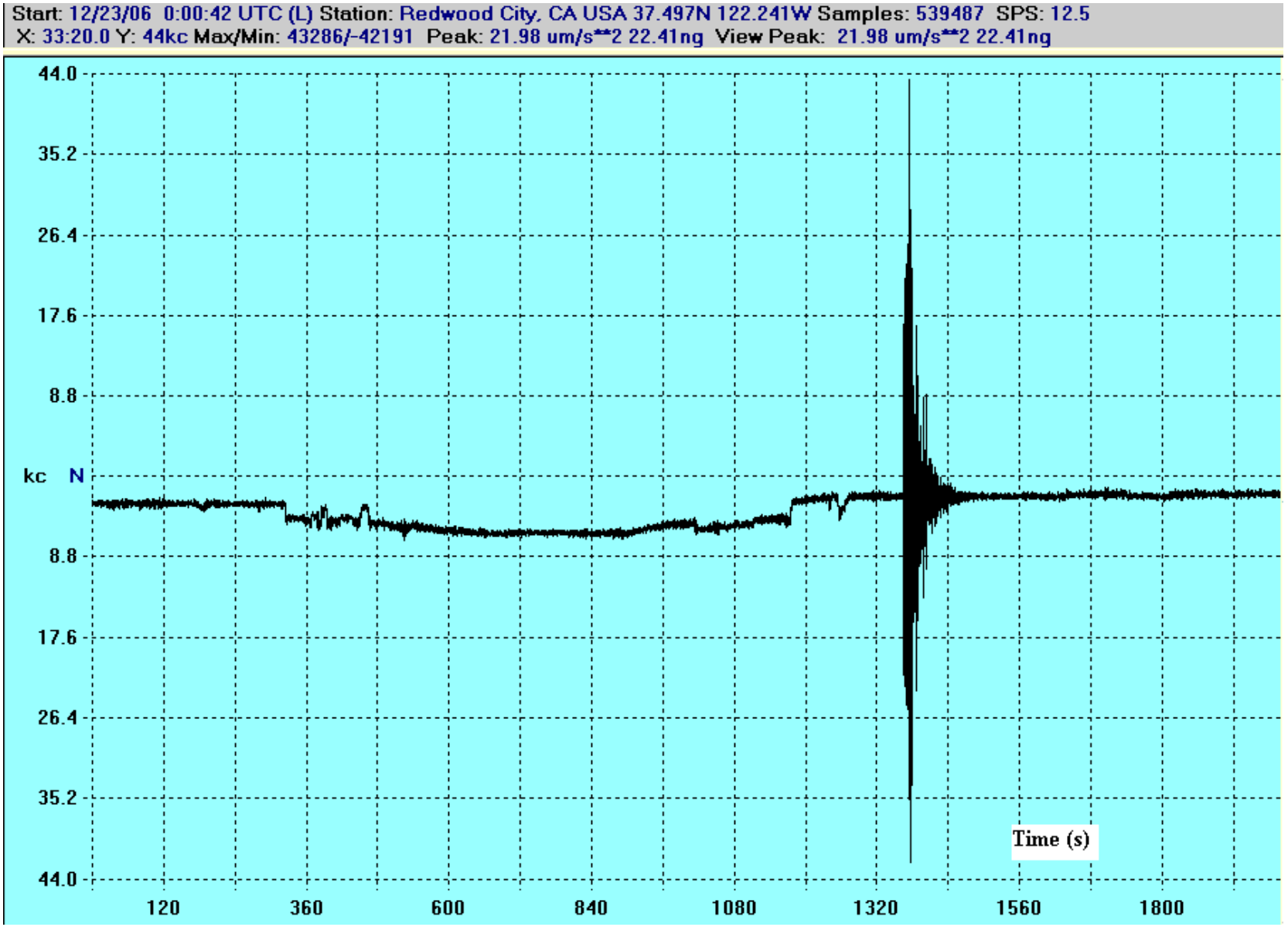

Figure 10. Highlighted (short-time) region of Fig. 9, showing the offset that just precedes the earthquake. Could the offset be a precursor to the earthquake?

One of the obvious questions that comes to mind from Fig. 10 is the following: could the offset be a precursor to the earthquake, or was it just coincidental? Only with extensive data analysis from an array of VolksMeters that have looked at many such earthquakes-could there ever be an answer to this question. The question is not likely to have surfaced on the basis of instruments using velocity sensors, as illustrated in Fig. 11.

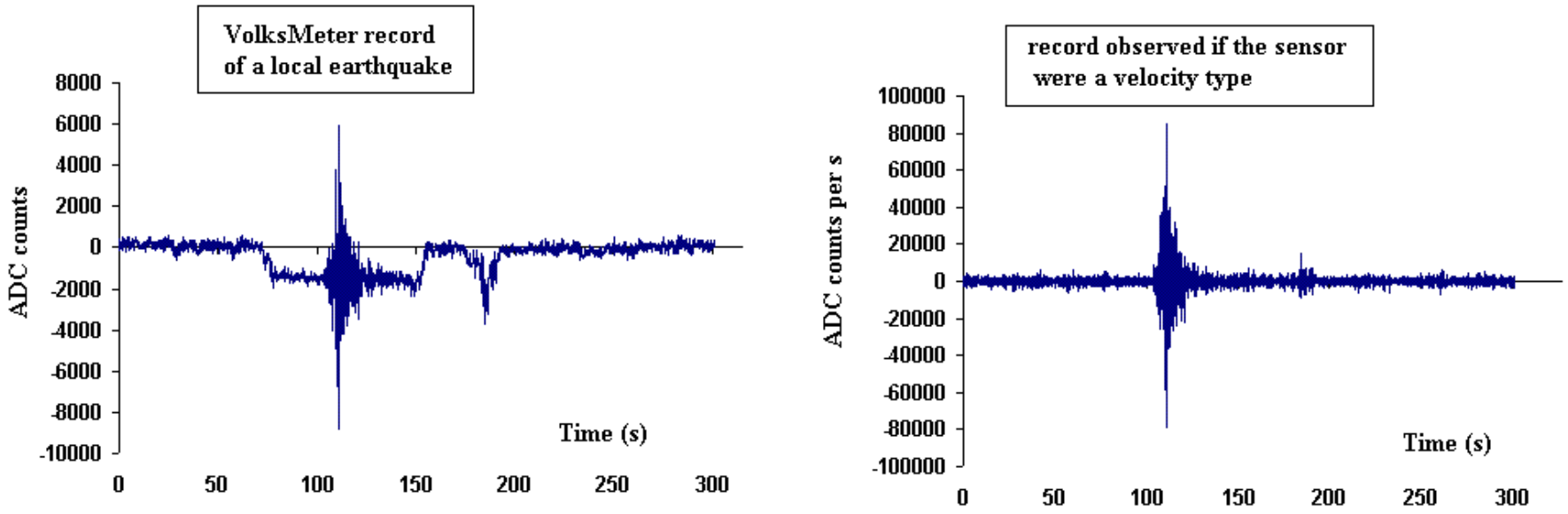

Figure 11. Illustration of why offset precursors are not likely to be discovered by conventional seismographs.

5 Estimate of teleseismic earthquake magnitudes

The following empirical expression long ago became the standard means for quickly estimating the (surface) magnitude of a teleseismic earthquake.

$$M_s = \text{Log}\,\frac{A}{T} + 1.66\,\text{Log}\,\Delta + 3.3 \qquad (1)$$

where A is the displacement magnitude of the peak in μm and T is the period in s (nominally in the vicinity of 20 s). Delta is the angular separation in degrees between the earthquake and the seismometer, and the logarithm is to the base 10.

5.1 Estimate of amplitude

It is shown in the theory section that the amplitude of the ground motion is given by

$$A = \frac{g}{\omega^2}\theta_0 \qquad (2)$$

where θ_0 is the amplitude in radians of the pendulum deflection -**if** $\omega < \omega_0$. If the condition should not be met (which it is not for local earthquakes), then a correction for the transfer function must be made, in accord with the left-graph of the following figure.

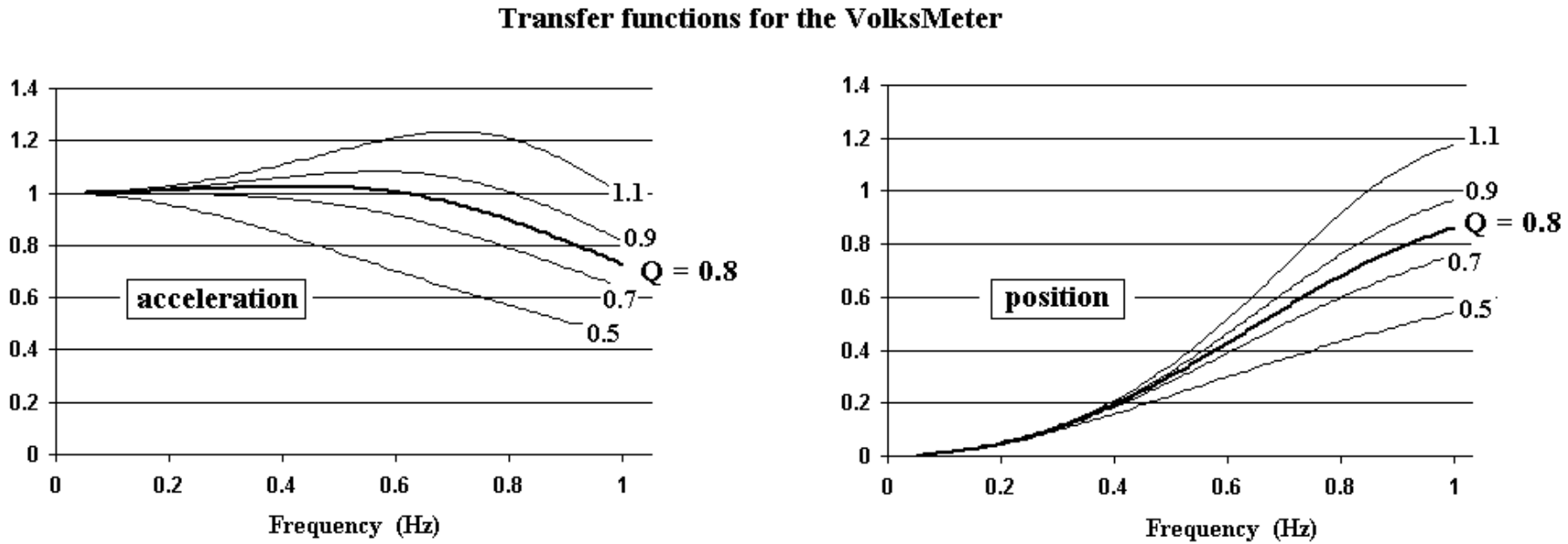

Figure 12. Plots of the transfer function T_F for the VolksMeter. The left graph is for acceleration, and the right graph for position illustrates how the pendulum's displacement is less than ground displacement for $\omega < \omega_0$.

The nominal value for the Q of the VolksMeter is 0.8, but the curves show how the transfer function varies with Q in the vicinity of 0.8. It is seen that for every case, no correction for T_F is required for teleseismic earthquakes, where the frequency of the peak motion is less than 0.1 Hz.

It is worth noting that the amplitude of pendulum motion is given for these cases by

$$A_{pend.} = \frac{g}{\omega_0^2}\theta_0 \qquad (3)$$

In other words, in the case of teleseismic surface waves, the pendulum amplitude is smaller than the ground amplitude by the ratio ω^2/ω_0^2. This ratio is consistent with the well-known reason for efforts to lengthen the period of seismometers-to increase the sensitivity according to the square of the period. For the pendulum this is nothing other than sensitivity being proportional to its length, since the period of a simple pendulum is proportional to the square root of its length.

We now use equations (1) and (2) to estimate the magnitude of the Samoa earthquake shown in Fig. 4. We first expand the x-scale as shown in Fig. 13

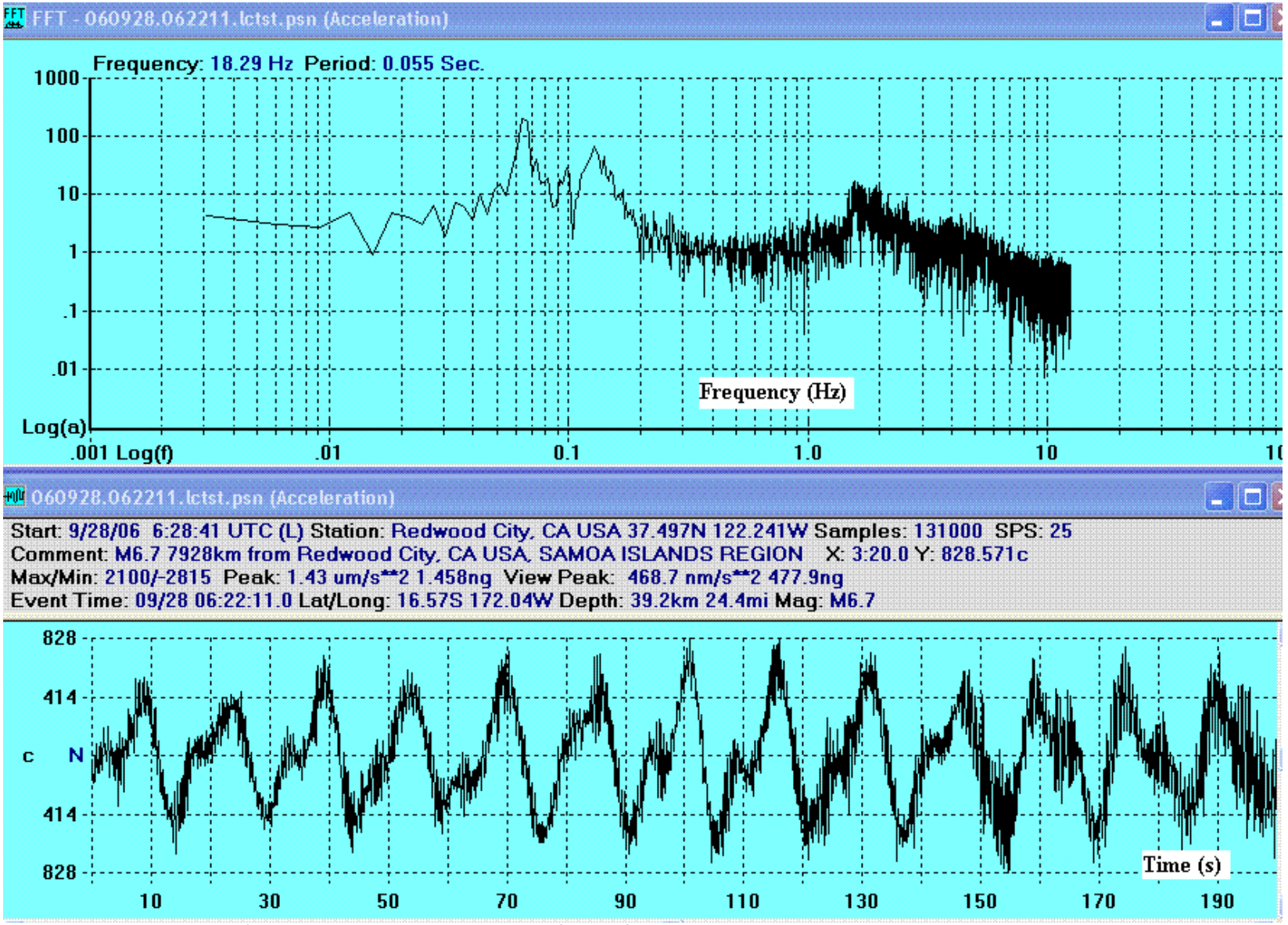

Figure 13. Scale expansion of Fig. 4 raw data to pick out the peak of the surface waves.

The peak pendulum displacement is estimated to be 720 ADC counts, and from the spectrum the period is found to be 15 s. For the instrument that produced the record, the calibration constant was estimated to be 1.25×10^9 cts/rad. Thus the peak ground displacement is estimated from eqns (1) and (2) to be 32 μm. From the figure it is noted that the distance between Samoa and Redwood City is 7928 km. Dividing this distance by 40,000 km (earth's circumference) and multiplying by 360 gives $\Delta = 71$. Substitution into eq. (1) results in a final surface magnitude estimate of 6.7. The magnitude value indicated for the Samoa earthquake by the USGS is 6.9, but this is the moment magnitude M_w, which typically differs somewhat from the estimates based on surface wave amplitudes.

6 Comparison with broadband commercial instruments

VolksMeter performance compares surprisingly well with broadband instruments costing five to twenty times as much. Some examples are now provided.

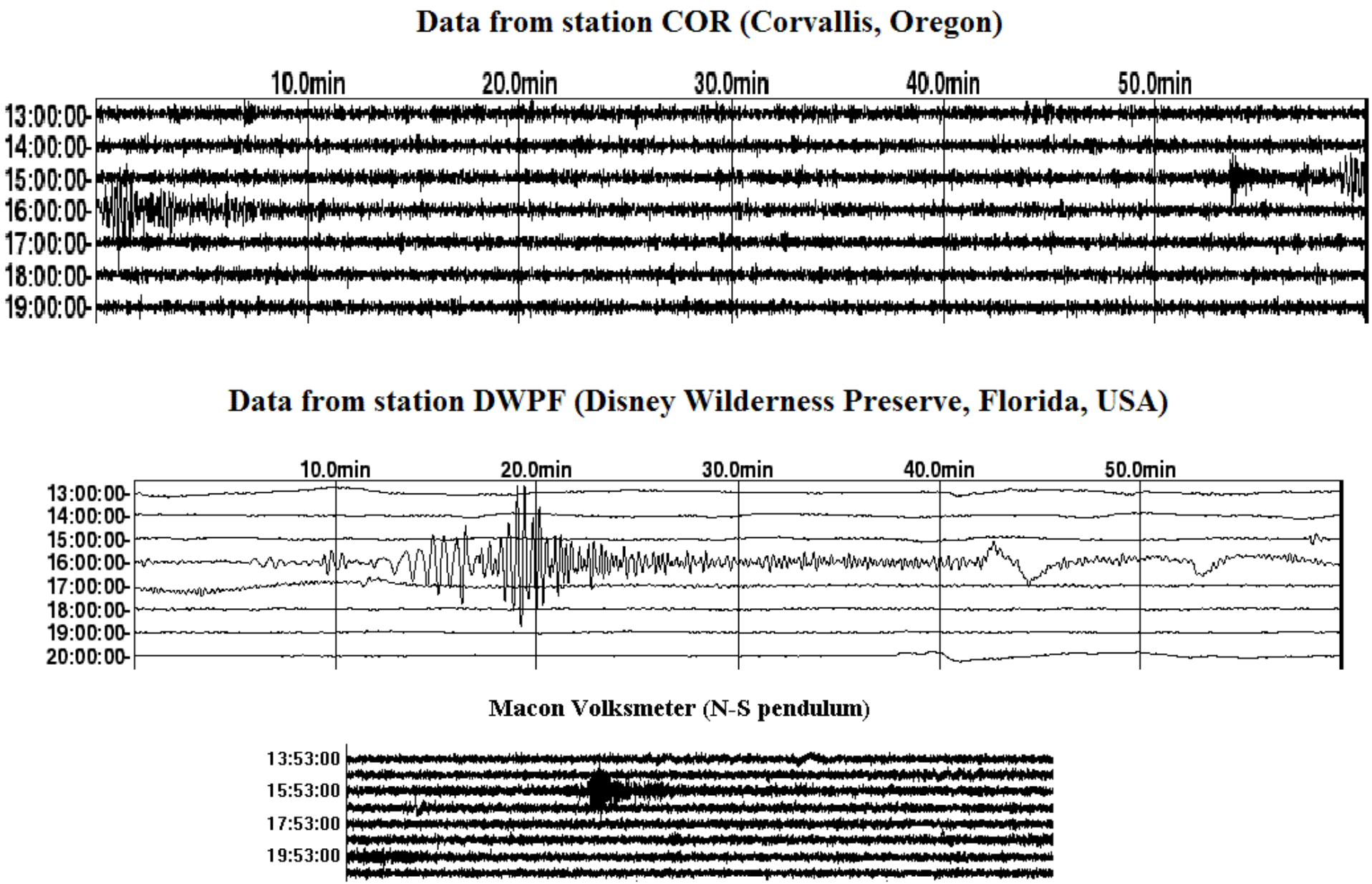

Figure 14. Comparison of the VolksMeter to STS-1 instruments- response to the Mag. 5.7 British Columbia earthquake of 9 January 2007.

Both the VolksMeter helicord and the Corvallis helicord are `broadband' (no filter), whereas the record from the Florida site is `long-period', bandpass filtered from 1 mHz to 40 mHz.

The reason the VolksMeter compares this well is because the largest spectral component in the waves is at 0.16 Hz (6.2 s period) as shown in Fig. 15.

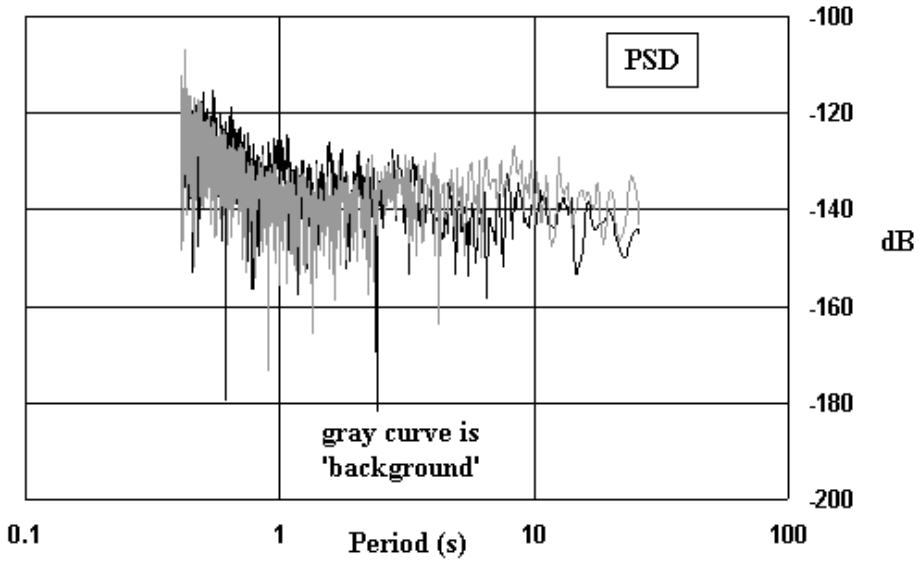

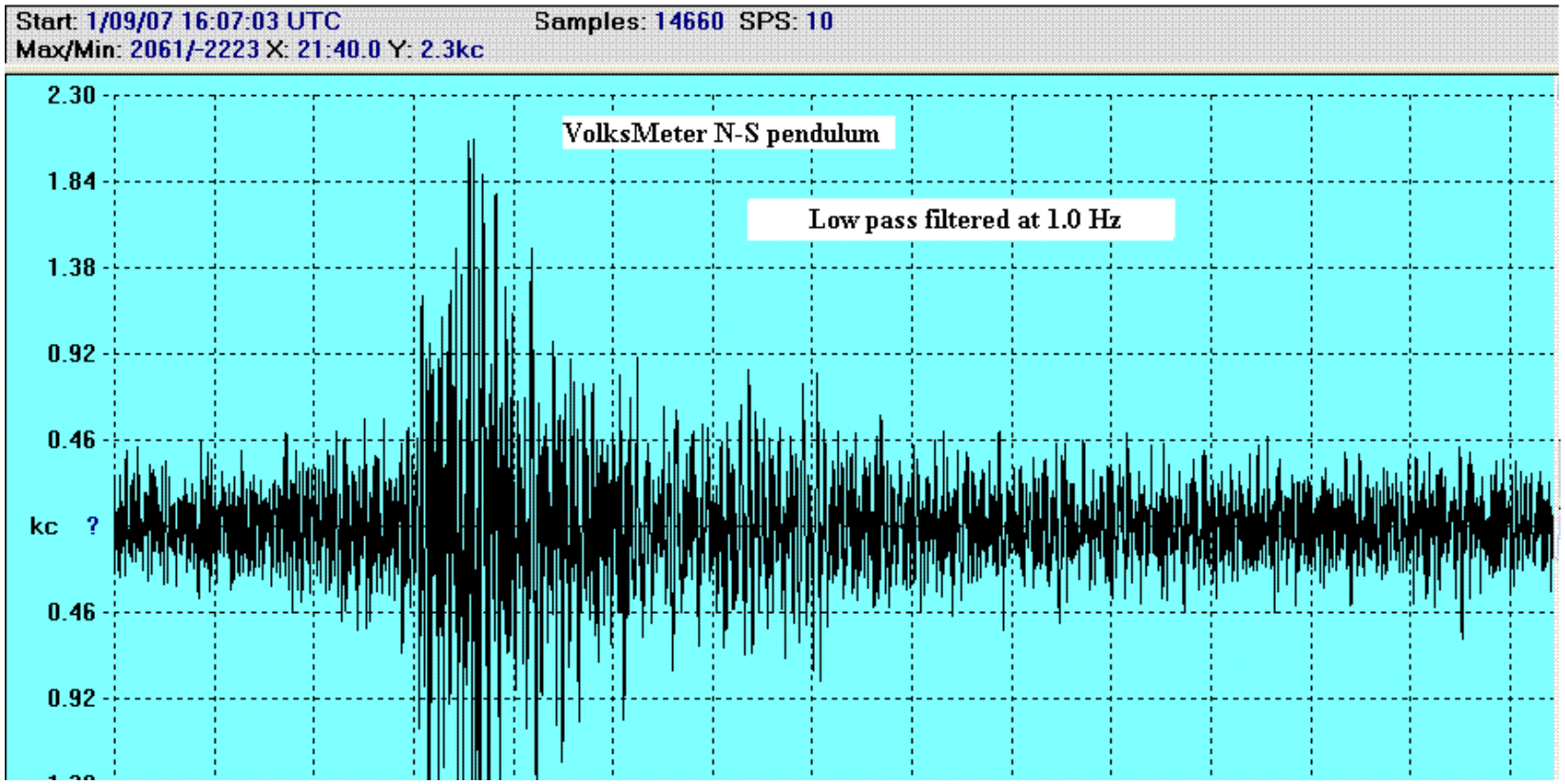

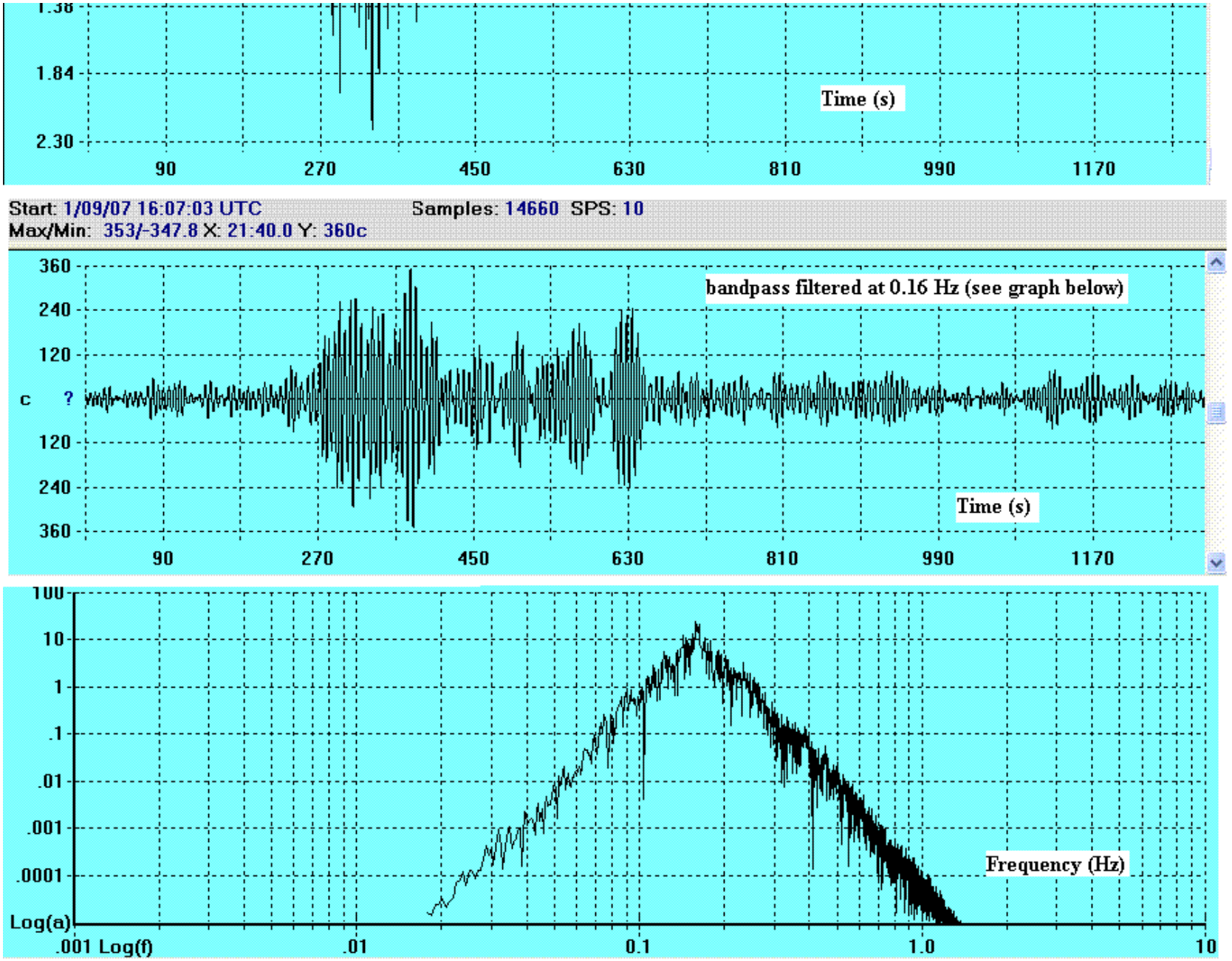

Figure 15. Figure to illustrate the spectral properties of the waves received from the British Columbia earthquake in Macon, Georgia.

Had the largest spectral component been at lower frequency (typically 50 mHz for waves from teleseismic events) the greater sensitivity of the STS-1 would have been more evident.

It should be noted that these comparisons are not rigorous, since the STS-1 records correspond to vertical ground motion whereas that of the Volksmeter is horizontal. Nevertheless, what is illustrated by these comparisons is the surprisingly high level of broadband performance realized by the VolksMeter-when it comes to earthquake monitoring. We will see in the material

which follows, concerned with very low frequencies (realm of eigenmode oscillations of the Earth), evidence to support the belief that the VolksMeter here outperforms the STS-1 and all other common commercial seismometers that use velocity sensors.

7 Instrument Equivalent Noise

The theory section of this manual shows a graph for the noise equivalent power spectral density of the VolksMeter, obtained by caging the pendulum. That graph is shown in comparison to another graph of earth noise (Berger et al.) Users of the VolksMeter are encouraged to generate some PSD's corresponding to their quietest records. By this means they can assess the noise quality of their environment. A representative example of earth noise in Macon, Georgia is provided by Fig. 16a.

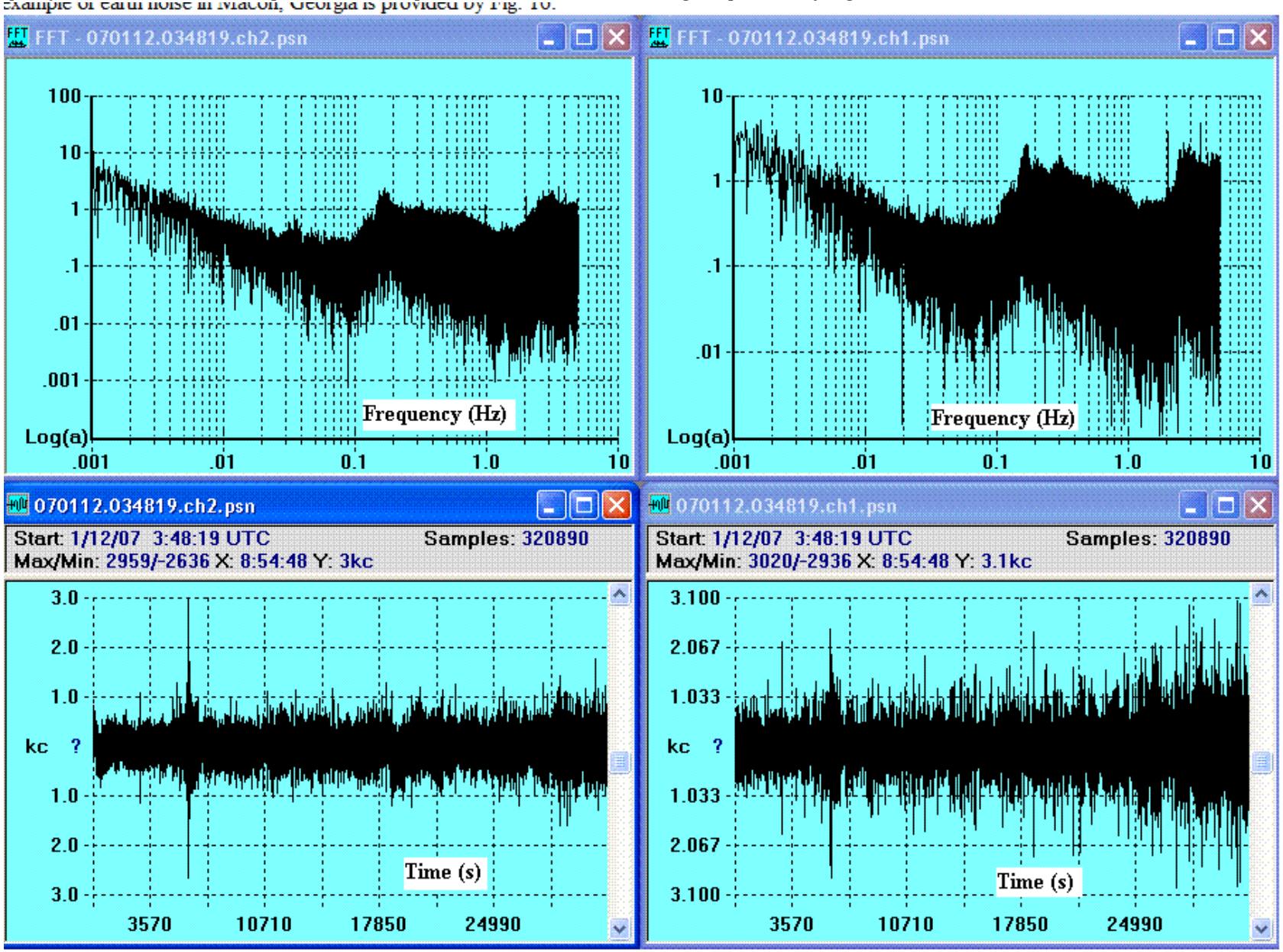

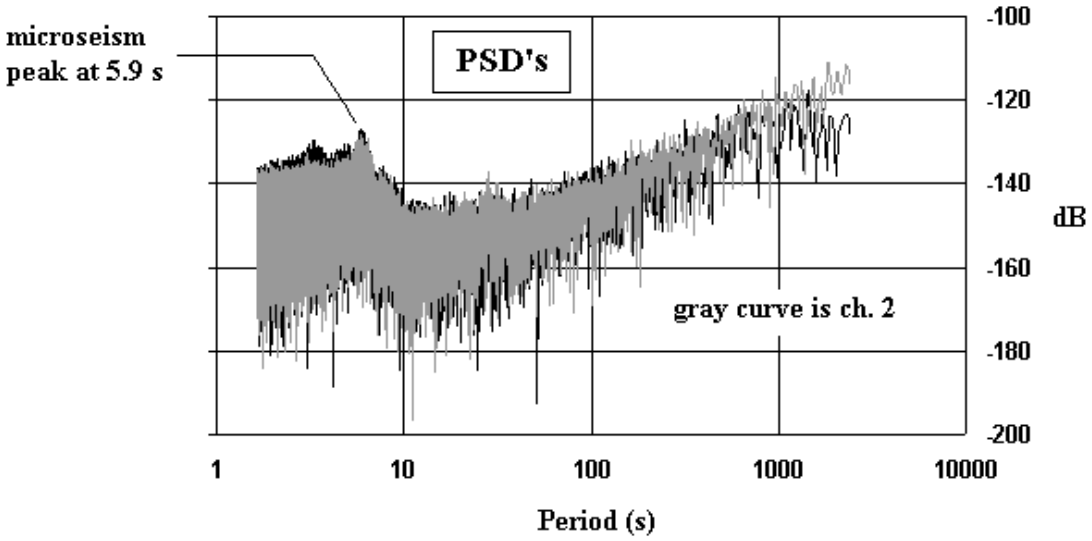

Figure 16a. Records thought to approximately represent the earth-noise state of Macon, Georgia at near quietest times.

The spike that is evident in the record of both pendulums is a high-frequency event, and may be due to a train. As seen in Fig. 16b, high-pass filtering at 0.1 Hz does not significantly change the shape of the spike.

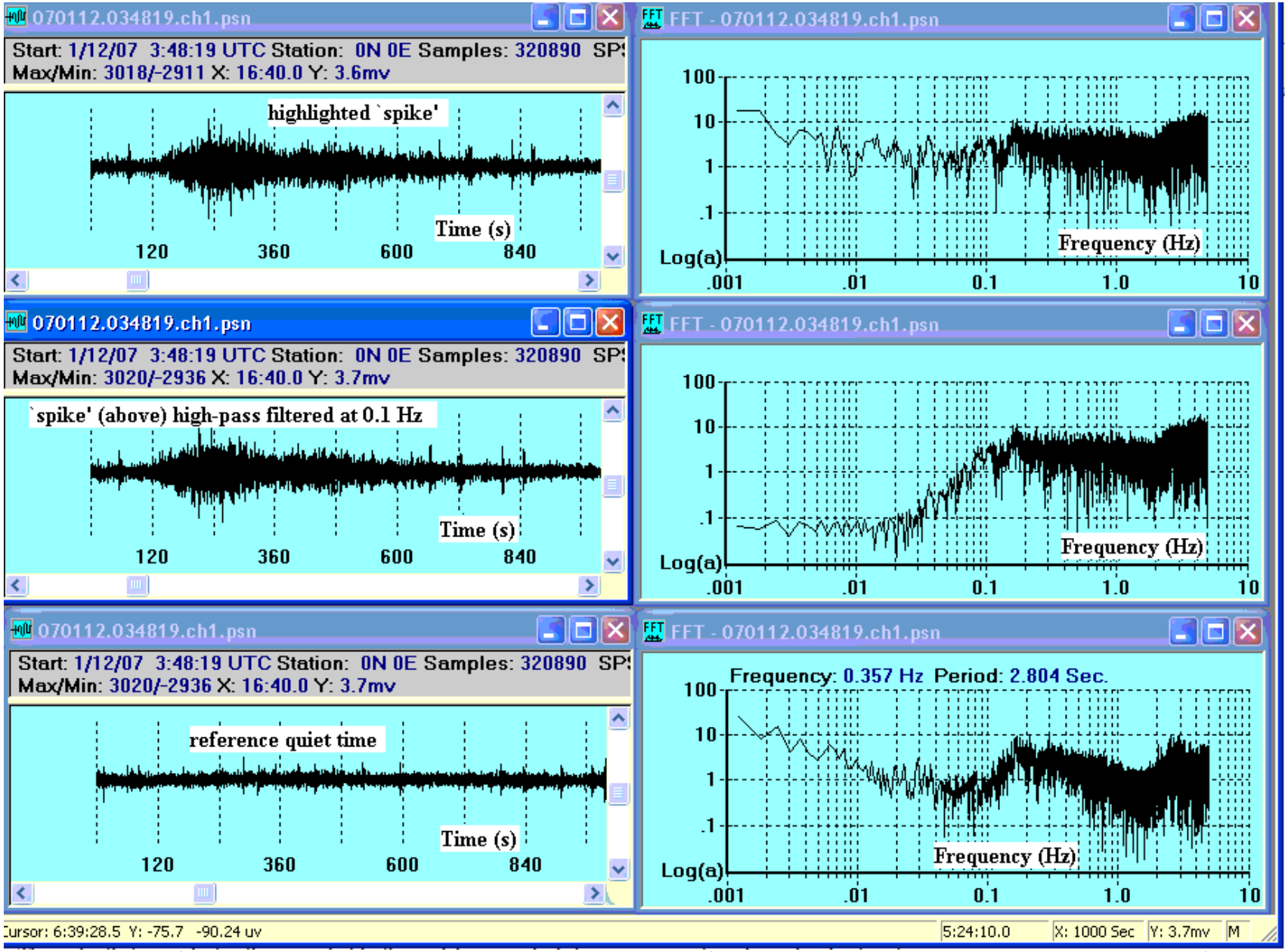

Figure 16b. Region of the Fig.16a record highlighting the spike thought to be the result of a train's passage. For a given temporal record shown on the left, its associated spectrum is shown immediately to the right.

The reference (bottom) record corresponds to a middle-piece of ch.1 in Fig. 16a.

File translated from T_EX by T_TH, version 1.95.

On 12 Jan 2007, 16:15.